

Multiwavelength observations of Mkn 421 in a flaring state in Jan/Feb 2001 with HEGRA and RXTE

D. Horns¹, A. Kohnle¹, F. A. Aharonian¹, for the HEGRA Collaboration, and R. A. Remillard²

¹Max-Planck-Institut für Kernphysik, Postfach 10 39 80, D-69029 Heidelberg, Germany

²Center for Space Research, Massachusetts Institute of Technology, Cambridge, MA 02139-4307, USA

Abstract. The blazar type active galaxy Mkn 421 was observed during an active phase in January and February 2001 with the X-ray satellite RXTE and with the ground-based HEGRA system of TeV Cherenkov telescopes. Observations were coordinated to allow for simultaneous data taking. Both instruments observed time-dependent variations of the flux and the spectral shape in X-rays and TeV γ -rays. Variability and correlations in the TeV and X-ray bands are observed on timescales of hours.

1 Introduction

The extragalactic object Mkn 421 is an X-ray selected BL-Lac-type AGN. The source is known for its strong variability in the X-ray and TeV-band (Gaidos et al. (1996)). During an active period in January and February 2001 the source was observed simultaneously with the instruments onboard the Rossi X-ray timing explorer (RXTE) and the HEGRA air Cherenkov telescopes.

2 Data analyses

2.1 TeV data

The HEGRA system of imaging air Cherenkov telescopes consists of 5 telescopes collecting air Cherenkov light with a 8.5 m² tessellated spherical mirror each. The light is detected in a hexagonal matrix of Photomultiplier tubes in the prime focus. Using advanced techniques (topological triggering scheme and multi-telescope coincidences) the influence of night sky background light and Cherenkov light by muons as major cause of instrumental background have been reduced considerable in comparison to a stand-alone telescope. The angular resolution for single events is better than 0.1°, the

relative energy resolution for the method used in this analysis is 20%.

The TeV data were taken during clear moonless nights. The air Cherenkov telescopes detect photon induced air showers with an energy threshold of 500 GeV for observations close to the zenith. The threshold increases to about 850 GeV for observations at 30° distance to the zenith. The data selected for spectral analyses is constrained to a maximum distance of 30° to the zenith whereas the lightcurves are derived from data extending to 45° distance to the zenith. The methods for data reconstruction and spectral analyses are described in Aharonian et al. (1999).

In total 220 hours of data have been collected during the observations in the year 2001. 170 hours have been analysed and are described in these proceedings Kohnle et al. (2001). The data used here are constrained to the time of simultaneous observation with the RXTE satellite from Jan 24, 2001 until Feb 4, 2001 and comprise in total 70 hours of observations under good conditions (low atmospheric extinction, no cloud coverage and stable detector performance).

2.2 X-ray data

The Proportional Counter Array (PCA) and the High Energy X-ray Timing Explorer (HEXTE) onboard the RXTE satellite observed from Jan-24 until Feb-4 (2001) Mkn 421 for a total exposure of 88 ksec (24.4 hrs). For details of the individual pointings see Table 1. After selection of data using the standard screening criteria (elevation of more than 10° above the limb of the Earth, offset to the position of the source less than 0.05°, low contamination by electrons, at least 30 minutes since last passage through the Southern Atlantic Anomaly), 50 ksec (13.9 hrs) remain for data analyses.

The PCA is a spectrophotometer composed of five collimated proportional counter units (PCU). A collimator constrains the field of view to an angle of 1° at half-maximum. The detectors are sensitive to photons with energies from 2 to 60 keV. The effective area of each PCU peaks between 5 and 10 keV at 1000 cm² and drops off quickly towards higher en-

Begin and end of pointing			Γ	F_{2-20}^*	$\frac{\chi^2}{d.o.f.}$	Γ_1	Γ_2	$\frac{E_{break}}{keV}$	$\frac{\chi^2}{d.o.f.}$
24-01-01	01:04:50	01:29:15	2.28 ± 0.03	103.8	0.82	-	-	-	-
24-01-01	20:02:31	20:39:15	2.69 ± 0.03	59.3	0.71	-	-	-	-
25-01-01	15:06:23	16:15:15	2.40 ± 0.01	139.1	1.31	2.32	2.53	9.2	0.69
26-01-01	11:44:00	15:59:15	2.42 ± 0.01	130.4	2.10	2.37	2.67	12.3	0.66
27-01-01	12:01:41	16:36:15	2.62 ± 0.01	115.2	1.50	2.58	2.81	10.5	0.66
28-01-01	13:29:46	14:01:15	2.70 ± 0.01	87.8	1.20	-	-	-	-
29-01-01	13:15:59	14:06:15	2.60 ± 0.02	110.8	2.02	2.54	2.79	10.0	0.53
30-01-01	06:40:26	07:10:15	2.53 ± 0.02	79.3	0.93	-	-	-	-
30-01-01	08:27:48	08:57:15	2.56 ± 0.03	89.4	0.71	-	-	-	-
31-01-01	00:11:49	07:00:15	2.46 ± 0.01	158.6	2.96	2.42	2.71	12.6	0.69
01-02-01	06:28:35	06:55:15	2.20 ± 0.03	134.1	1.24	2.17	2.51	13.0	0.83
02-02-01	12:54:33	15:01:15	2.52 ± 0.01	77.8	1.10	-	-	-	-
03-02-01	12:19:44	13:15:15	2.48 ± 0.01	149.9	2.75	2.41	2.93	12.2	0.95
04-02-01	04:26:36	04:47:15	2.63 ± 0.02	103.5	0.72	-	-	-	-
04-02-01	06:01:36	06:36:15	2.57 ± 0.02	99.3	0.92	-	-	-	-

* In units of 10^{-11} erg cm $^{-2}$ s $^{-1}$

Table 1. Summary of observations and spectral fits to the X-ray data. The error on the spectral index gives the 67 % confidence range ($\Delta\chi^2 = 1$). Note that most of the observations are in accordance with a pure power law model. However, the energy spectra during the remaining observations are described better by a broken power law. The typical errors on the photon index before the break is 0.02 and after the break 0.07. The error on E_{break} is usually smaller than 2 keV.

ergies reaching 100 cm 2 between 20 and 30 keV. For higher energy photons two clusters of NaI/CsI scintillation detectors are mounted on the satellite (HEXTE clusters). Each cluster consists of 4 NaI/CsI phoswich scintillation detectors with a total efficient area of 800 cm 2 for photons with energies between 20 and 100 keV. More details on the instruments are given in Rothschild et al. (1998).

The realtime data have been extracted using the FTOOLS 5.0.4 package. Background estimates for the PCUs were determined with the pcabackest v2.1e using a background model for bright sources. Response matrices for the PCUs were calculated with the pcarsp v7.10 for the PCA and with hxtsrp v3.1 for the HEXTE clusters respectively. Due to a failure in the Propane layer of PCU0 and marginal operation time for the PCU1,3 and 4, only the top layer of PCU2 has been used for the analyses. The Scintillator#3 of the HEXTE cluster B has been excluded from the analyses due to a failure in the readout. The background estimates for the HEXTE observation have been calculated from observations of a separate sky region. The average count rate in PCU2 was 94 cts/s, the background according to the model was 14 cts/s. The maximum signal count rate was 137 cts/s and the minimum signal count rate was 34 cts/s. The respective average count rate detected by the HEXTE-clusters was 14 cts/s with an average background count rate of 180 cts/s.

Spectral analyses were performed using the XSPEC package in its version 11.0. Contemporaneous data taken from the Crab Nebula and pulsar were used to estimate the systematic error on individual bins of the energy spectra to be 10 %. Using the same data set, a normalization factor was determined to connect the PCA and HEXTE energy spectra smoothly. The HEXTE flux is scaled by a factor of 1/0.773 to obtain a continuous energy spectrum. This value has been

used for fits to the combined spectral information of the PCA and the HEXTE clusters.

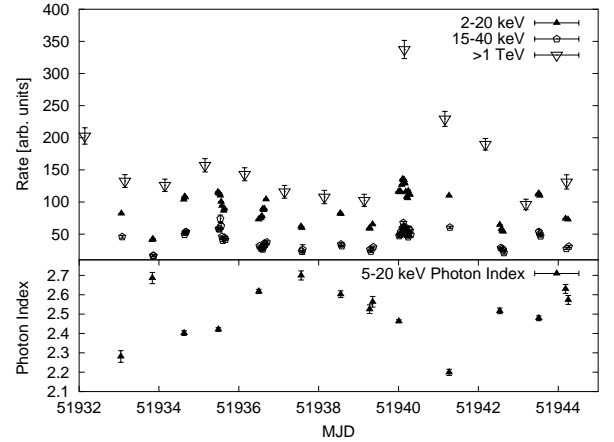


Fig. 1. For the period from Jan-23 until Feb-4 (2001) data from the RXTE satellite and from the HEGRA Cherenkov telescopes are displayed. The top panel shows the flux (in arbitrary units) in three energy intervals, the lower panel gives the photon index for the energy interval from 5 to 20 keV obtained with the PCA onboard the RXTE satellite

The column density of hydrogen was assumed to be $2 \cdot 10^{22}$ cm $^{-2}$. We excluded the energy range below 5 keV from the fit because of systematic deviations in the response of the PCU2 from the respective behaviour of other PCUs in this energy range. The upper end of the fit interval was determined individually by checking the significance above background. The HEXTE energy spectra above 15 keV were fit simultaneously together with the PCU energy spectra. Again, the upper end of the HEXTE energy spectra was chosen ac-

ording to the significance of the signal observed.

3 Results

3.1 Lightcurves

The diurnal flux above 1 TeV is shown in Figure 1 together with the X-ray flux averaged over 30 minutes. In general, the flux variability is comparable in the two energy ranges. For the truly simultaneous observations a tight correlation between TeV and X-ray flux variations is observed. However, the drop in the X-ray flux by a factor of two from the observations on MJD=51933.04 (Jan-24) to the flux detected in the subsequent pointing on MJD=51933.83 day was not seen in the TeV-observations starting three hours later. The peak flux detected on Jan-31 in the X-ray and TeV energy bands shows an increase of 40% with regards to the average X-ray flux level whereas the TeV flux increased by a factor of 2 with respect to the average flux value reaching the level of $(6.8 \pm 0.2) \cdot 10^{-11}$ photons/cm/s for energies above 1 TeV (corresponds to four times the flux of the Crab Nebula).

The general trend for the X-ray energy spectrum to become harder with increasing flux is seen throughout the observation period. However, there is one exception: the photon index decreases from 2.46 ± 0.01 to 2.20 ± 0.03 for the observations on Jan-31 to Feb-01, whereas the flux decreases slightly. This behaviour could be either attributed to a time lag for hard photons or to a second harder component that dominates.

The peak of the TeV flux observed in the night of Jan-31 was observed simultaneously with the RXTE instruments. For roughly 6 hours the X-ray flux increased and decreased smoothly with a relative amplitude of 20%. The TeV flux showed a completely different behaviour. The flux remained constant at a high level with $\approx 10^{-11}$ ph/cm²/s (six times the flux of the Crab Nebula) and dropped rapidly within 2 hours by a factor of 2. The hardness ratio and flux of X-ray photons showed a counter-clockwise behaviour where the soft photons lag the hard photons (acceleration faster than cooling) which is a surprising feature that is not consistent with the above mentioned behaviour observed over a few days. Further studies of discrete correlation functions are necessary to confirm possible lags in hard or soft photons and will be reported at the conference.

3.2 Energy spectra

The X-ray spectra are in most cases consistent with a pure power law. However, there is some evidence for deviations from a power law. Fitting the PCU and HEXTE data yield satisfactory χ^2 values for most cases (see Table 1). The observations on Feb-03 are not in agreement with a power law. A broken power law with the break energy at (12.2 ± 0.4) keV, a spectral index before the break of 2.41 ± 0.02 increasing by 0.5 at the break gives a $\chi^2/d.o.f$ of 0.95 (a single power law fit to the combined PCU and HEXTE data:

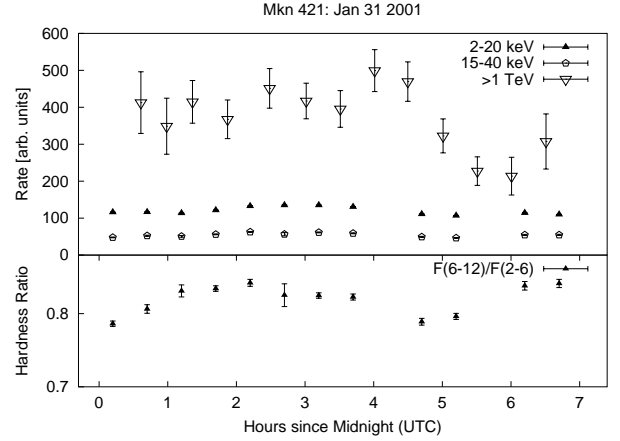


Fig. 2. During a long pointing of roughly 6 hours in the early morning of Jan-31 (2001), the source underwent a flare in X-ray and TeV emission. However, the temporal behaviour is different for the two energy bands: Whereas the flux increases and decreases smoothly, the TeV flux remains constant at a high level of 10^{-11} photons/cm²/s (six times the flux of the Crab Nebula) and drops by a factor of two within less than two hours. The lower panel shows the spectral hardness calculated from the X-ray flux detected between 2 and 6 keV and between 6 and 12 keV.

$\chi^2/d.o.f = 2.85$). Most energy spectra show a slight improvement of the χ^2 when fitting a broken power law with a break energy ranging from 9 to 13 keV. To estimate the position of the synchrotron peak (E_{sy}), an approximation of a synchrotron spectrum for a power-law electron distribution with an exponential cut-off has been fitted to the data (shown in Figure 3). The SED derived for the night with the highest flux (Jan-31), with the lowest flux (Jan-24) and the average over the whole data set have been each fitted with a function of the form $E^{-\alpha} \cdot E^{-\sqrt{E/E_m}}$. The power α has been fixed to the value 0.16 derived from fitting the average SED. E_m and the flux normalization have been left to vary. It is obvious, that E_{sy} is at lower energies than the observed energy interval setting an upper limit on E_{sy} to be smaller than 3 keV. The χ^2 value for the synchrotron model fit is acceptable $\chi^2/d.o.f. \approx 1 \dots 1.7$. However, models assuming different cutoffs give similar results and it is not possible to distinguish between the spectral shapes. It is certainly not possible to fit all the data with a pure power-law. More complex models are necessary and the best-fitting model is a broken power-law with a spectral steepening by $\Delta\Gamma = 0.3$ to $\Delta\Gamma = 0.5$.

4 Conclusions

The source activity of the Blazar-type AGN Mkn 421 has been studied in the X-ray and TeV energy band using data taken simultaneously with the HEGRA system of Cherenkov telescopes and the RXTE satellite. The PCA and HEXTE data were combined to study the X-ray energy spectrum above 5 keV up to 45 keV. The X-ray flux varied by more than a factor of 3 during the 11 days of data taking. The TeV

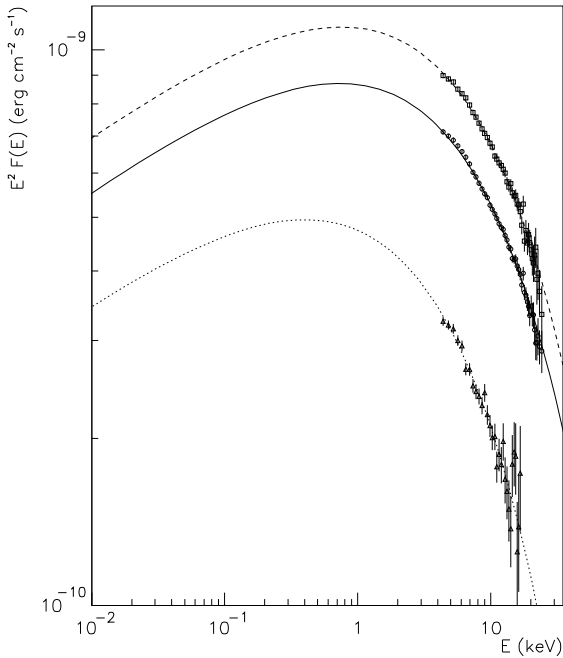


Fig. 3. Spectral fit of synchrotron models to the Mkn421 spectral energy distribution (SED) assuming a power law electron distribution with a cut-off using the δ -approximation. The slope has been kept fixed at a value of 0.16. The position of the synchrotron peak E_{sy} remains within the errors constant for the different flux levels (solid line: average spectrum, dashed line: data from Jan-31, dotted line: data from Jan-24). However, since the position of the synchrotron peak is not within the observed energy range, only an upper limit can be stated: $E_{sy} < 3$ keV.

flux showed comparable variations. The correlation between the X-ray and TeV flux is not always tight. The X-ray energy spectra are mostly consistent with pure power-laws with exceptions where broken power-laws give a satisfactory description of the data. The X-ray energy spectrum shows varying photon indices ranging from 2.2 to 2.7. The position of the synchrotron peak is below the energy range covered by RXTE ($E_{sy} < 3$ keV).

Acknowledgements. The authors acknowledge the support by the RXTE GOF. The support by the German Ministry for Research and Technology BMBF and by the Spanish Research Council CICYT is acknowledged. The staff of the ORM and the technical support of Heidelberg, Kiel, Munich, and Yerevan is gratefully acknowledged.

References

- Aharonian, F.A. et al., *A&A*, **349**, 11 (1999).
 Gaidos, J.A. et al., *Nature*, **383**, 319 (1996).
 Jahoda, K., Swank, J. H., Giles, A. B., Stark, M. J., Strohmayer, T., Zhang, W., & Morgan, E. H., *Proc. SPIE*, 2808, 59 (1996).
 Kohnle, A., Horns, D., Krawczynski, H. et al. *Proceedings of the 27th ICRC Hamburg* (2001).
 Rothschild, R. E. et al., *ApJ*, **496**, 538 (1998).